Contribution from the Department of Chemistry,
The University of Texas at Austin, Austin, Texas 78712

Mono-, Bis-, and Tris(phosphine) Derivatives of μ_3-Sulfido Hydrido Complexes of Rhodium and Iridium. Syntheses and X-ray Crystal Structures of 50-Electron $Rh_3(H)(\mu_3\text{-}S)_2(COD)_2(PMe_3)_3$ and $Ir_3(H)(\mu_3\text{-}S)_2(COD)_3(PMe_3)$ and 48-Electron $Ir_3(H)(\mu_3\text{-}S)_2(COD)_2(t\text{-}Bu_2PH)_2$ (COD = 1,5-Cyclooctadiene)

Theresa A. Bright, Richard A. Jones,* Stefan U. Koschmieder, and Christine M. Nunn

Received April 5, 1988

Reaction of hexamethyldisilthiane $[(Me_3Si)_2S]$ with $[Rh(COD)Cl]_2$ in the presence of excess PMe_3 in THF at −78 °C produces a deep red solution from which the 50-electron red crystalline complex $Rh_3(H)(\mu_3\text{-}S)_2(COD)_2(PMe_3)_3$ (**1**) may be isolated (82%) (COD = 1,5-cyclooctadiene). A similar reaction with $[Ir(COD)Cl]_2$ produces 50-electron purple crystalline $Ir_3(H)(\mu_3\text{-}S)_2(COD)_3(PMe_3)$ (**2**) (58%). Reaction of $[Ir(COD)Cl]_2$ with NaSH in MeOH at −78 °C produces $Ir_3(H)(\mu_3\text{-}S)_2(COD)_3$ (**3**) (69%). Complex **3** may also be produced from the direct reaction of H_2S (1 atm) with $[Ir(COD)Cl]_2$ in MeOH at room temperature as well as by reaction of hexamethyldisilthiane with $[Ir(COD)Cl]_2$ in THF at −78 °C. Reaction of **3** with excess $t\text{-}Bu_2PH$ yields $Ir_3(H)(\mu_3\text{-}S)_2(COD)_2(t\text{-}Bu_2PH)_2$ (**4**). Both **3** and **4** may be considered as 48-electron clusters. The structures of **1**, **2**, and **4** have been determined by X-ray crystallography. In each case, the molecular framework consists of a triangle of three metal atoms capped on both faces by μ_3-S atoms. In **1**, a COD ligand is bound to two Rh atoms, while a third bears three PMe_3 ligands. One Rh–Rh distance is significantly longer than the other two [3.578 (2) vs 2.874 (1) and 2.904 (2) Å]. In **2**, a COD ligand is bound to each Ir atom and a single PMe_3 group is attached to one Ir atom. As in **1**, one Ir–Ir distance is much longer than the other two (3.614 (1) vs 2.809 (2) and 2.826 (1) Å). In **3**, a COD ligand is bound to each Ir atom, and in **4** one Ir is bound to two $t\text{-}Bu_2PH$ groups. Crystal data for **1**: $C_{25}H_{48}P_3Rh_3S_2$, M_n = 814.43, orthorhombic, $P2_12_12_1$ (No. 19), a = 11.525 (5) Å, b = 16.325 (1) Å, c = 17.586 (5) Å, V = 3308.6 (5) Å^3, D_c = 1.635 g·cm^{-3}, Z = 4, μ(Mo Kα) = 17.35 cm^{-1}. Refinement of 1788 reflections ($I > 3\sigma(I)$) out of 2582 unique observed reflections ($3° < 2\theta < 50°$) gave R and R_w values of 0.0615 and 0.0770, respectively. Crystal data for **2**: $C_{27}H_{39}Ir_3S_2P$, M_n = 1035.31, monoclinic, $P2_1/n$ (No. 14), a = 16.916 (3) Å, b = 8.853 (3) Å, c = 19.648 (6) Å, β = 105.37 (2)°, V = 2837.0 (5) Å^3, D_c = 2.424 g·cm^{-3}, Z = 4, μ(Mo Kα) = 142.00 cm^{-1}. Refinement of 3042 reflections ($I > 3\sigma(I)$) out of 5551 unique observed reflections ($3° < 2\theta < 50°$) gave R and R_w values of 0.0574 and 0.0647, respectively. Crystal data for **4**: $C_{32}H_{63}Ir_3P_2S_2$, M_n = 1188.58, triclinic, $P\bar{1}$ (No. 2), a = 10.849 (3) Å, b = 20.423 (3) Å, c = 10.577 (6) Å, α = 101.09 (2)°, β = 115.22 (2)°, γ = 81.52 (2)°, V = 2074.7 (5) Å^3, D_c = 1.902 g·cm^{-3}, Z = 2, μ(Mo Kα) = 97.57 cm^{-1}. Refinement of 3544 reflections ($I > 3\sigma(I)$) out of 5421 unique observed reflections ($3° < 2\theta < 46°$) gave R and R_w values of 0.0444 and 0.0521, respectively.

Introduction

There is widespread interest in transition-metal complexes containing S^{2-}, SH^-, or SR^- as ligands since they behave as models for biological systems[1] as well as hydrodesulfurization catalysts.[2] The majority of these complexes contain firmly bound ligands such as cyclopentadienyl, CO, or anionic moieties SR^- or halide. In order to develop the chemistry of transition-metal sulfur complexes, we have undertaken a broad study of d-block transition-metal SH^- or sulfido (S^{2-}) complexes bearing weakly bound ligands such as PR_3, AsR_3, or alkenes.[3] Such complexes may well exhibit unusual and interesting new reactivity modes, since their ligands should be easily displaced.

Results

The transformations observed in this study are summarized in Schemes I and II together with prior related studies. The 48-electron hydrido μ_3-sulfido cluster $Rh_3(H)(COD)_3(\mu_3\text{-}S)_2$ (COD = 1,5-cyclooctadiene) shown in Scheme I may be prepared from the reaction of NaSH with $[Rh(COD)Cl]_2$ in methanol.[4] This complex reacts with $t\text{-}Bu_2PH$ to give the unusual phosphine-substituted complex $Rh_3(H)(COD)_2(\mu_3\text{-}S)_2(t\text{-}Bu_2PH)_2$, in which only one COD ligand is replaced. Both of the remaining COD ligands may be replaced with CO to give $Rh_3(H)(CO)_4(\mu_3\text{-}S)_2(t\text{-}Bu_2PH)_2$ (Scheme I). There are several noteworthy features of these complexes. One is simply the fact that very few other Rh_3 sulfido (μ_3-S) complexes are known. The pattern of COD replacement by phosphine followed by CO substitution was also interesting. In addition, very unusual ^1H NMR spectra for the unique hydride ligand in the phosphine and CO derivatives were observed. These discoveries prompted us to further explore the chemistry of this new class of compounds.

Since several groups of workers[5,6] have reported the use of hexamethyldisilthiane $[(Me_3Si)_2S]$ as a means of preparing transition-metal sulfido complexes, we investigated reactions of it with $[M(COD)Cl]_2$ (M = Rh, Ir). The reaction of $(Me_3Si)_2S$ with $[Rh(COD)Cl]_2$ and excess PMe_3 in THF gives dark red, crystalline $Rh_3(H)(\mu_3\text{-}S)_2(COD)_2(PMe_3)_3$ (**1**) in high yield (82%). In the absence of excess PMe_3, $Rh_3(H)(\mu_3\text{-}S)_2(COD)_3$ is obtained in 77% yield. In contrast, the reaction of $(Me_3Si)_2S$ with $[Ir(COD)Cl]_2$ and PMe_3 in THF gives the mono(phosphine) derivative $Ir_3(H)(\mu_3\text{-}S)_2(COD)_3(PMe_3)$ (**2**) in good yield (58%) (Scheme II). In the absence of PMe_3, the complex $Ir_3(H)(\mu_3\text{-}S)_2(COD)_3$ (**3**) may be isolated in 69% yield. We also investigated the reaction of **3** with $t\text{-}Bu_2PH$. This reaction produces the Ir complex $Ir_3(H)(\mu_3\text{-}S)_2(COD)_2(t\text{-}Bu_2PH)_2$ (**4**), which is isostructural with its Rh analogue. During the course of our studies on the iridium complexes, we discovered two other routes to **3**. One is from the reaction of $[Ir(COD)Cl]_2$ with NaSH in methanol. This route is analogous to the one originally employed for $Rh_3(H)(\mu_3\text{-}S)_2(COD)_3$. However, a simple method for the preparation of **3** is by bubbling H_2S (1 atm) through a solution of $[Ir(COD)Cl]_2$ in methanol. This gives the product in 65% yield after recrystallization from toluene (Scheme II).

There are several noteworthy features of the new complexes. In particular, compounds **1** and **2** are formally 50-electron species

(1) See for example: Vahrenkamp, H. *Angew. Chem., Int. Ed. Engl.* **1975**, *14*, 322 and references therein. Newton, W. E., Otsuka, S., Eds. *Molybdenum Chemistry of Biological Significance*; Plenum: New York, 1980. Lovenberg, W., Ed. *Iron-Sulfur Proteins*; Academic: New York, 1973, 1974, 1976; Vols. 1–3. Steifel, E. I. *Prog. Inorg. Chem.* **1977**, *22*, 1.
(2) Shah, V. K.; Brill, W. J. *Proc. Natl. Acad. Sci. U.S.A.* **1977**, *74*, 3249. Coucovanis, D. *Acc. Chem. Res.* **1981**, *14*, 201.
(3) Arif, A. M.; Hefner, J. G.; Jones, R. A. *J. Am. Chem. Soc.* **1986**, *108*, 1701.
(4) Arif, A. M.; Hefner, J. G.; Jones, R. A.; Koschmieder, S. U. *Polyhedron* **1988**, *7*, 561.
(5) Do, Y.; Simhon, E. D.; Holm, R. H. *Inorg. Chem.* **1985**, *24*, 1831.
(6) Money, J. K.; Huffman, J. C.; Christou, G. *Inorg. Chem.* **1985**, *24*, 3297.

0020-1669/88/1327-3819$01.50/0

Scheme I. Trinuclear Rhodium Complexes, Showing the Unique Hydrides in Their Proposed Locations (See Text)

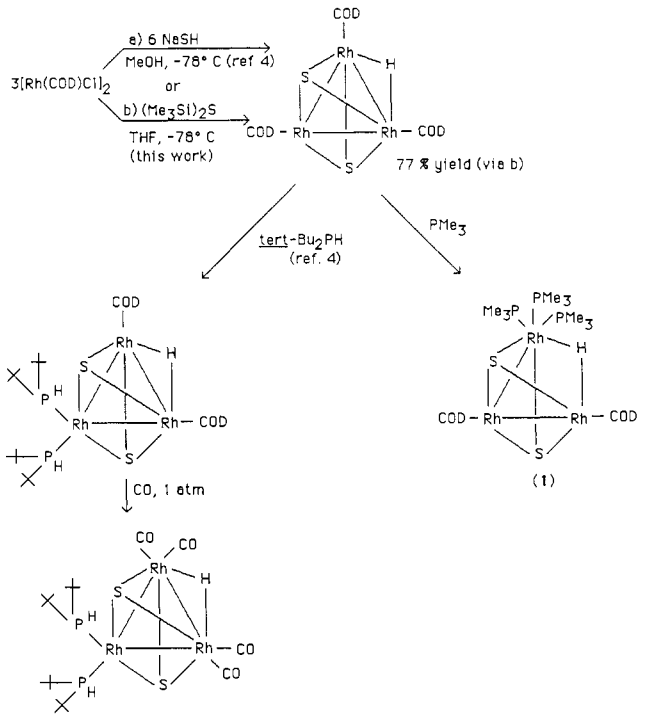

Scheme II. Trinuclear Iridium Complexes, Showing the Unique Hydrides in Their Proposed Locations (See Text)

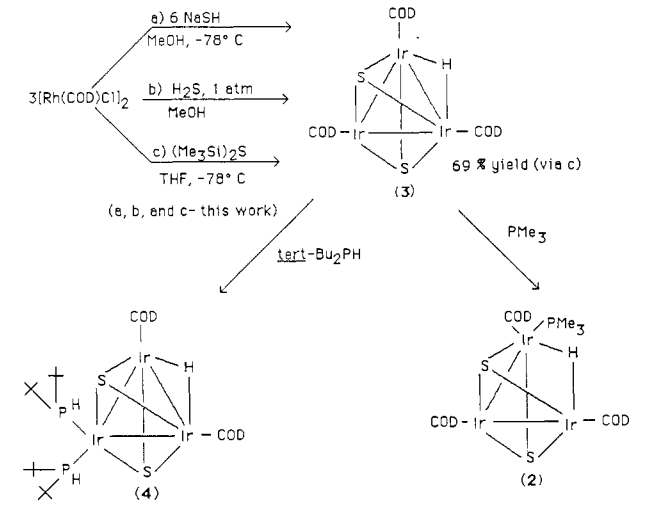

having 2 electrons in excess of the 48 normally required for a closed trinuclear cluster.[7] A number of 50-electron trinuclear cluster compounds are known. The geometries of the metal frameworks of these clusters vary considerably. One extreme form is the open linear arrangement such as that found in $[Rh_3\{\mu\text{-}(Ph_2PCH_2)_2PPh\}_2(H)_2(\mu\text{-}Cl)_2(CO)_2]^+$ and related compounds.[8] A considerable number of 50-electron clusters have triangular frameworks with two metal–metal bonds and a third interaction that is considerably longer than a bonding distance. An example of this type of cluster is $Fe_3(\mu\text{-}S)_2(CO)_9$.[9] There are a few examples of clusters with more than 48 electrons that have all short, clearly bonding metal–metal distances. Examples of these include $Co_3(\mu_3\text{-}PPh)(CO)_9$ (49 electrons),[10] $Co_3(\mu\text{-}SEt)_5(\mu\text{-}CO)(CO)_3$ (50 electrons),[11] and $Rh_3(\mu\text{-}PPh_2)_3(\mu\text{-}Cl)_2(\mu\text{-}CO)(CO)_3$ (50 electrons).[12] Another category of trinuclear clusters with 50 electrons also exists. These have metal–metal interactions that are long but not too long to be nonbonding distances. Examples of this type of compound are $Rh_3(\mu\text{-}PPh_2)_3(CO)_7$ and $Rh_3(\mu\text{-}PPh_2)_3(CO)_6(PPh_2H)$.[13] Compounds **1** and **2** are the type of cluster with two metal–metal bonds and a third nonbonding interaction.

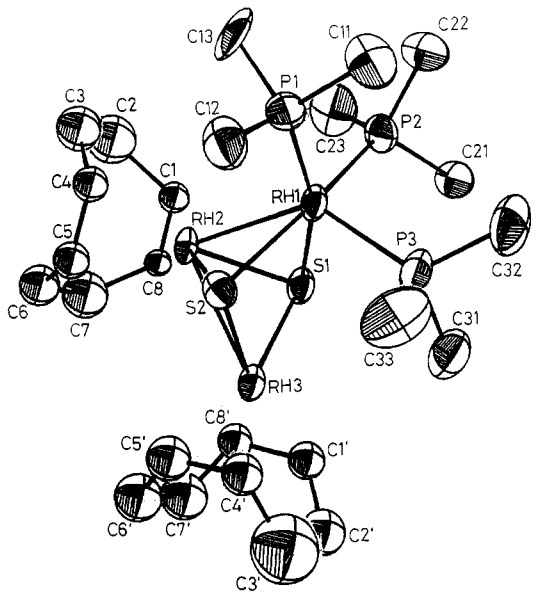

Figure 1. ORTEP view of **1**, showing the atom-numbering scheme. Atoms are shown at the 50% probability level.

Other unusual features of the new compounds include the molecular geometry of **1**, which exhibits an unusual pattern of phosphine substitution in which all three PMe_3 ligands are bound to a single Rh atom. Variable-temperature NMR data indicate that one PMe_3 group undergoes a rapid dissociative exchange process in solution. For **2**, NMR data indicate that two isomers are present in solution. Although all the complexes have been thoroughly characterized by spectroscopic (IR, NMR) techniques and in the case of **1**, **2**, and **4** by single-crystal X-ray crystallography, the location of the unique hydride ligand both in solution and in the solid state for each compound is by no means unequivocal.

Apart from our initial report[4] describing μ_3-S-bridged sulfido clusters of Rh_3, there are relatively few others of Rh_3 or Ir_3 that have been described. A related system is that of the carbonylate anions $[M_3(CO)_6(\mu_3\text{-}X)_2]^-$ (M = Rh, Ir; X = S, Se) reported by Garlaschelli, Sironi, and co-workers.[14,15] Also of related interest is the recent report by Cotton and co-workers of the iridium complex $Ir_3(COD)_3(\mu_3\text{-}O)_2(\mu_2\text{-}I)$,[16] which is a 50-electron complex and is isostructural with **3** and $Rh_3(H)(COD)_3(\mu_3\text{-}S)_2$.[4] In addition, a number of heterobimetallic sulfido-bridged Rh and Ir complexes are known. For example, Rauchfuss and co-workers

(7) See for example: Lauher, J. W. *J. Am. Chem. Soc.* **1978**, *100*, 5305 and references therein.
(8) Balch, A. L.; Linehan, J. C.; Olmstead, M. M. *Inorg. Chem.* **1986**, *25*, 3937.
(9) Wei, C. H.; Dahl, L. F. *Inorg. Chem.* **1965**, *4*, 493.
(10) Beurich, H.; Madach, T.; Richter, F.; Vahrenkamp, H. *Angew. Chem., Int. Ed. Engl.* **1979**, *18*, 690.
(11) Klumpp, E.; Marko, L.; Bor, G., *Chem. Ber.* **1964**, *97*, 926. Wei, C. H.; Dahl, L. *J. Am. Chem. Soc.* **1968**, *90*, 3960.
(12) Haines, R. J.; Steen, N. D. C. T.; English, R. B. *J. Chem. Soc., Dalton Trans.* **1983**, 2229.
(13) Haines, R. J.; Steen, N. D. C. T.; English, R. B. *J. Chem. Soc., Dalton Trans.* **1984**, 515.
(14) Galli, D.; Garlaschelli, L.; Ciani, G.; Fumagalli, A.; Martinengo, S.; Sironi, A. *J. Chem. Soc., Dalton Trans.* **1984**, 55.
(15) Pergola, R. D.; Garlaschelli, L.; Martinengo, S.; Demartin, F.; Manassero, M.; Sansoni, M. *J. Chem. Soc., Dalton Trans.* **1986**, 2463.
(16) Cotton, F. A.; Lahuerta, P.; Sanau, M.; Schwotzer, W. *J. Am. Chem. Soc.* **1985**, *107*, 8284.

Table I. Crystal Structure Parameters for Complexes **1**, **2**, and **4**

chem formula	$C_{25}H_{48}Rh_3S_2P_3$	$C_{27}H_{39}Ir_3S_2P_1$	$C_{32}H_{63}Ir_3S_2P_2$
a, Å	11.525 (5)	16.916 (3)	10.848 (2)
b, Å	16.325 (1)	8.852 (3)	20.422 (5)
c, Å	17.586 (5)	19.647 (6)	10.576 (3)
α, deg	90	90	101.09 (2)
β, deg	90	105.37 (2)	115.22 (2)
γ, deg	90	90	81.52 (2)
V, Å^3	3308.6 (5)	2837.0 (5)	2074.7 (5)
Z	4	4	2
M_r	814.426	1035.314	1149.78
space group	$P2_12_12_1$	$P2_1/n$	$P\bar{1}$
temp, °C	23 ± 2	23 ± 2	23 ± 2
radiation (λ, Å)	Mo Kα (0.71073)	Mo Kα (0.71073)	Mo Kα (0.71073)
D_c, g·cm^{-3}	1.635	2.424	1.902
μ(Mo Kα), cm^{-1}	17.349	141.997	97.574
transmission coeff	93.667–98.341	20.514–99.716	22.521–99.949
R^a	0.0615	0.0574	0.0444
$R_w{}^a$	0.0770	0.0647	0.0521

[a] R and R_w are defined as $R = \sum||F_o| - |F_c||/\sum|F_o|$ and $R_w = [\sum w(|F_o| - |F_c|)^2/\sum w(|F_o|^2]^{1/2}$.

Table II. Selected Bond Lengths (Å) and Angles (deg) for **1**[a]

Rh(1)–Rh(2)	2.874 (1)	Rh(3)–S(2)	2.330 (3)
Rh(1)–Rh(3)	3.578 (2)	Rh(3)–S(1)	2.350 (3)
Rh(2)–Rh(3)	2.904 (2)	Rh(2)–C(1)	2.11 (1)
Rh(1)–S(1)	2.435 (7)	Rh(2)–C(4)	2.19 (1)
Rh(1)–S(2)	2.449 (8)	Rh(2)–C(5)	2.195 (1)
Rh(1)–P(1)	2.297 (8)	Rh(2)–C(18)	2.11 (1)
Rh(1)–P(2)	2.30 (1)	Rh(3)–C(1)′	2.19 (1)
Rh(1)–P(3)	2.399 (9)	Rh(3)–C(4)′	2.06 (1)
Rh(2)–S(1)	2.381 (3)	Rh(3)–C(5)′	2.17 (2)
Rh(2)–S(2)	2.384 (4)	Rh(3)–C(8)′	2.107 (1)
Rh(1)–Rh(2)–Rh(3)	76.50 (4)	Rh(3)–Rh(2)–S(1)	51.6 (1)
Rh(2)–Rh(1)–S(1)	52.50 (6)	Rh(3)–Rh(2)–S(2)	51.15 (8)
Rh(2)–Rh(1)–S(2)	52.48 (9)	Rh(3)–Rh(2)–C(1)	132.7 (3)
Rh(2)–Rh(1)–P(1)	108.81 (9)	Rh(3)–Rh(2)–C(4)	134.9 (4)
Rh(2)–Rh(1)–P(2)	112.0 (1)	Rh(3)–Rh(2)–C(5)	104.3 (4)
Rh(2)–Rh(1)–P(3)	133.0 (1)	Rh(3)–Rh(2)–C(8)	102.6 (3)
S(1)–Rh(1)–S(2)	77.2 (1)	S(1)–Rh(2)–S(2)	79.5 (1)
S(1)–Rh(1)–P(1)	161.3 (1)	S(1)–Rh(2)–C(1)	95.9 (3)
S(1)–Rh(1)–P(2)	89.7 (1)	S(1)–Rh(2)–C(4)	164.5 (4)
S(1)–Rh(1)–P(3)	95.6 (1)	S(1)–Rh(2)–C(5)	154.2 (4)
S(2)–Rh(1)–P(1)	92.2 (1)	S(1)–Rh(2)–C(8)	92.2 (3)
S(2)–Rh(1)–P(2)	164.0 (1)	S(2)–Rh(2)–C(1)	168.9 (3)
S(2)–Rh(1)–P(3)	91.0 (2)	S(2)–Rh(2)–C(4)	95.6 (4)
P(1)–Rh(1)–P(2)	97.8 (2)	S(2)–Rh(2)–C(5)	91.8 (4)
P(1)–Rh(1)–P(3)	100.0 (2)	S(2)–Rh(2)–C(8)	151.5 (3)
P(2)–Rh(1)–P(3)	99.5 (2)	Rh(1)–P(1)–C(11)	119 (1)
Rh(2)–Rh(3)–S(1)	52.62 (7)	S(1)–Rh(3)–S(2)	81.3 (1)
Rh(2)–Rh(3)–S(2)	52.8 (1)	S(1)–Rh(3)–C(1)′	94.7 (4)
Rh(2)–Rh(3)–C(1)′	134.5 (4)	S(1)–Rh(3)–C(4)′	158.7 (4)
Rh(2)–Rh(3)–C(4)′	139.3 (4)	S(1)–Rh(3)–C(5)′	160.0 (4)
Rh(2)–Rh(3)–C(5)′	108.3 (4)	S(1)–Rh(3)–C(8)′	96.8 (5)
Rh(2)–Rh(3)–C(8)′	105.3 (4)	S(2)–Rh(3)–C(4)′	95.4 (4)

[a] Numbers in parentheses are estimated standard deviations in the least significant digits. A complete listing is available in the supplementary material.

Table III. Positional Parameters for **1**[a]

atom	x	y	z	B, Å^2
Rh(1)	1.3053 (2)	−0.4350 (1)	1.0696 (2)	2.94 (4)
Rh(2)	0.9990 (2)	0.0457 (1)	0.9365 (2)	2.79 (4)
Rh(3)	1.0528 (2)	−0.0589 (1)	0.8077 (2)	2.99 (5)
S(1)	1.5106 (6)	−0.4001 (3)	1.0672 (5)	3.3 (2)
S(2)	1.3847 (6)	−0.5178 (4)	1.1735 (5)	3.3 (2)
P(1)	1.1365 (6)	−0.5098 (4)	1.0670 (7)	4.0 (2)
P(2)	1.2797 (8)	−0.3661 (4)	0.9571 (6)	4.4 (2)
P(3)	1.2506 (8)	−0.3290 (5)	1.1571 (6)	4.4 (2)
C(1)	1.574 (2)	−0.559 (2)	0.955 (2)	2.9 (5)*
C(1)′	1.678 (3)	−0.343 (2)	1.213 (2)	3.9 (6)*
C(2)	1.534 (4)	−0.650 (2)	0.919 (3)	7 (1)*
C(2)′	1.677 (3)	−0.318 (2)	1.297 (2)	5.7 (9)*
C(3)	1.456 (3)	−0.698 (2)	0.966 (2)	5.8 (9)*
C(3)′	1.615 (5)	−0.375 (4)	1.353 (4)	12 (2)*
C(4)	1.440 (2)	−0.672 (2)	1.050 (2)	3.3 (6)*
C(4)′	1.545 (2)	−0.443 (2)	1.309 (2)	4.2 (6)*
C(5)′	1.603 (3)	−0.518 (2)	1.287 (2)	4.9 (8)*
C(5)	1.539 (3)	−0.670 (2)	1.104 (2)	3.7 (6)*
C(6)′	1.733 (3)	−0.528 (2)	1.287 (2)	6.1 (9)*
C(6)	1.663 (3)	−0.692 (2)	1.084 (2)	4.8 (8)*
C(7)	1.736 (4)	−0.630 (2)	1.041 (3)	7 (1)*
C(7)′	1.803 (3)	−0.465 (2)	1.243 (2)	6.4 (9)*
C(8)	1.661 (2)	−0.555 (1)	1.008 (2)	2.2 (5)*
C(8)′	1.732 (2)	−0.422 (2)	1.187 (2)	3.6 (6)*
C(11)	0.993 (3)	−0.453 (2)	1.066 (3)	6.2 (8)
C(12)	1.110 (3)	−0.574 (2)	1.151 (2)	5.5 (9)
C(13)	1.128 (3)	−0.577 (2)	0.986 (3)	7 (1)
C(21)	1.331 (3)	−0.259 (2)	0.958 (2)	5.1 (9)
C(22)	1.139 (3)	−0.353 (2)	0.913 (3)	8 (1)
C(23)	1.367 (4)	−0.406 (2)	0.881 (2)	7 (1)
C(31)	1.367 (3)	−0.256 (2)	1.184 (3)	7 (1)
C(32)	1.130 (3)	−0.257 (2)	1.134 (3)	7 (1)
C(33)	1.198 (4)	−0.365 (3)	1.251 (3)	8 (1)

[a] Starred values indicate atoms were refined isotropically. Anisotropically refined atoms are given in the form of the isotropic equivalent thermal parameter defined as $(4/3)[a^2B(1,1) + b^2B(2,2) + c^2B(3,3) + ab(\cos\gamma)B(1,2) + ac(\cos\beta)B(1,3) + bc(\cos\alpha)B(2,3)]$.

recently described the synthesis of complexes of the type $MS_4[Rh(COD)]_2$ (M = Mo, W).[17]

Synthesis of $Rh_3(H)(\mu_3\text{-}S)_2(COD)_2(PMe_3)_3$ (1). Reaction of hexamethyldisilthiane $[(Me_3Si)_2S]$ with $[Rh(COD)Cl]_2$ in THF at −78 °C gives an orange solution that turns dark red upon addition of excess PMe_3. From this solution, dark red $Rh_3(H)(\mu_3\text{-}S)_2(COD)_2(PMe_3)_3$ (**1**) may be obtained in high yield following recrystallization from hexane. The complex is moderately air stable and does not decompose in hydrocarbon solutions over several days. NMR (^1H, ^{31}P) spectral data for **1** is not in accord with the structure of the compound as found in the solid state. At 35 °C the 300-MHz ^1H NMR spectrum for **1** has resonances that may be assigned to COD and PMe_3, but no high-field signal for a hydride is observed. However, on cooling of the sample solution to 20 °C, a doublet of triplets is observed at high field. The resonance becomes sharper at −20 °C and broadens on further cooling (−80 °C). On sample warming, the resonance collapses at around 35 °C and no signal can be observed up to 80 °C. The coupling constant associated with the triplet is 11.5 Hz, while that of the doublet is 184.8 Hz. The coupling constants remain unchanged when the spectrum is obtained at 500 MHz, thus indicating that the large separation between the triplets is due to coupling and not to two chemically inequivalent protons. It seems reasonable to assume that the triplets are due to coupling to rhodium and the doublet is due to phosphorus. However, when one considers the solid-state structure of the complex, it is clear that this resonance is deceptively simple. The

(17) Howard, K. E.; Rauchfuss, T. B.; Rheingold, A. L. *J. Am. Chem. Soc.* **1986**, *108*, 297.

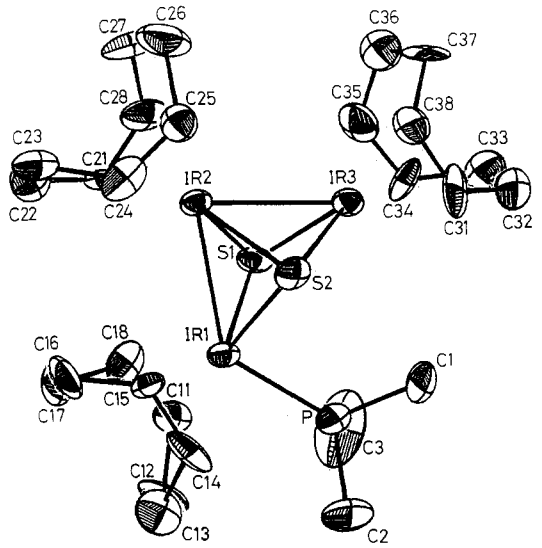

Figure 2. ORTEP view of **2**, showing the atom-numbering scheme. Atoms are shown at the 50% probability level.

Table IV. Selected Bond Lengths (Å) and Angles (deg) for **2**[a]

Ir(2)–Ir(3)	2.809 (2)	Ir(2)–S(2)	2.359 (7)
Ir(1)–Ir(2)	2.826 (1)	Ir(2)–C(21)	2.15 (3)
Ir(1)–Ir(3)	3.614 (1)	Ir(2)–C(24)	2.11 (3)
Ir(1)–S(1)	2.374 (6)	Ir(2)–C(25)	2.11 (3)
Ir(1)–S(2)	2.391 (6)	Ir(2)–C(28)	2.24 (3)
Ir(1)–P	2.394 (9)	Ir(3)–S(1)	2.356 (7)
Ir(1)–C(11)	2.18 (3)	Ir(3)–S(2)	2.364 (7)
Ir(1)–C(14)	2.18 (3)	Ir(3)–C(31)	2.11 (3)
Ir(1)–C(15)	2.13 (3)	Ir(3)–C(34)	2.06 (3)
Ir(1)–C(18)	2.18 (3)	Ir(3)–C(35)	2.15 (3)
Ir(2)–S(1)	2.367 (7)	Ir(3)–C(38)	2.12 (3)
Ir(2)–Ir(1)–S(1)	53.3 (2)	Ir(1)–S(1)–Ir(2)	73.2 (2)
Ir(2)–Ir(1)–S(2)	53.0 (2)	Ir(1)–S(1)–Ir(3)	99.7 (3)
Ir(2)–Ir(1)–P	131.5 (2)	Ir(2)–S(1)–Ir(3)	73.0 (2)
Ir(2)–Ir(1)–C(11)	125.1 (7)	Ir(1)–Ir(2)–Ir(3)	79.80 (4)
Ir(2)–Ir(1)–C(14)	127.7 (8)	Ir(1)–Ir(2)–S(1)	53.5 (1)
Ir(2)–Ir(1)–C(15)	90.4 (6)	Ir(1)–Ir(2)–S(2)	54.0 (2)
Ir(2)–Ir(1)–C(18)	90.5 (7)	Ir(2)–Ir(3)–S(1)	53.7 (2)
S(1)–Ir(1)–S(2)	77.9 (2)	Ir(2)–Ir(3)–S(2)	53.4 (2)
S(1)–Ir(1)–P	91.8 (3)	S(1)–Ir(2)–S(2)	78.7 (3)
S(1)–Ir(1)–C(11)	97.3 (8)	Ir(3)–Ir(2)–S(1)	53.3 (2)
S(1)–Ir(1)–C(14)	177.3 (8)	Ir(3)–Ir(2)–S(2)	53.6 (2)
S(1)–Ir(1)–C(15)	141.8 (6)	S(1)–Ir(3)–S(2)	78.8 (2)
S(1)–Ir(1)–C(18)	89.4 (8)	S(2)–Ir(1)–P	91.2 (3)
Ir(1)–S(2)–Ir(2)	73.0 (2)	Ir(2)–S(2)–Ir(3)	73.0 (2)
Ir(1)–S(2)–Ir(3)	98.9 (3)		

[a] Numbers in parentheses are estimated standard deviations in the least significant digits. A complete listing is available in the supplementary material.

$^{31}P\{^1H\}$NMR spectrum of **1** is again inconsistent with the solid-state structure. At 300 MHz and ambient temperature, no clearly defined signal can be observed. However, on cooling of the sample to −10 °C, two very broad doublets are observed. On further sample cooling, these resonances sharpen considerably, and at −50 °C, they appear as two doublets (δ 2.89, $^1J_{Rh-P}$ = 118.7 Hz; δ −5.62, $^1J_{Rh-P}$ = 118.2 Hz, $^2J_{P-P}$ = 19.6 Hz). In addition, there is a very broad signal at ca. δ −40 ($\Delta w_{1/2}$ = 360 Hz). The sharp resonances are indicative of two nonequivalent PMe_3 groups bound to one Rh atom. We assume that the broad hump is due to the third PMe_3 ligand, which is undergoing a dissociative exchange process that is rapid on the NMR time scale. There is no signal for free PMe_3 (δ − 62.9).

X-ray Structure of 1. The complex crystallizes in the orthorhombic space group $P2_12_12_1$ with four molecules in the unit cell. A view of the molecule is shown in Figure 1. Crystallographic data are collected in Table I, and selected bond lengths and angles are in Table II. Positional parameters are given in Table III.

Table V. Positional Parameters for **2**[a]

atom	x	y	z	B, Å^2
Ir(1)	0.87202 (5)	0.5500 (1)	0.12680 (5)	2.34 (2)
Ir(2)	1.02468 (6)	0.6700 (1)	0.20287 (5)	2.33 (2)
Ir(3)	1.00110 (6)	0.4507 (1)	0.29894 (5)	2.44 (2)
S(1)	0.9933 (4)	0.4117 (8)	0.1787 (3)	2.7 (1)
S(2)	0.9076 (4)	0.6419 (8)	0.2455 (3)	2.7 (1)
P	0.7874 (5)	0.357 (1)	0.1560 (4)	3.5 (2)
C(1)	0.794 (2)	0.327 (5)	0.249 (2)	7.2 (9)
C(2)	0.674 (2)	0.376 (6)	0.122 (2)	8 (1)
C(3)	0.803 (3)	0.166 (5)	0.122 (3)	11 (2)
C(11)	0.847 (2)	0.450 (4)	0.022 (1)	3.9 (7)
C(12)	0.757 (2)	0.475 (4)	−0.023 (2)	4.7 (8)
C(13)	0.720 (2)	0.615 (4)	0.000 (2)	5.1 (9)
C(14)	0.761 (2)	0.674 (4)	0.074 (1)	4.2 (7)
C(15)	0.831 (1)	0.770 (3)	0.090 (11)	2.4 (5)
C(16)	0.864 (2)	0.833 (4)	0.032 (1)	4.8 (7)
C(17)	0.889 (2)	0.707 (4)	−0.014 (2)	4.7 (8)
C(18)	0.909 (2)	0.564 (4)	0.029 (1)	4.2 (6)
C(21)	1.099 (1)	0.689 (4)	0.130 (1)	3.2 (6)
C(22)	1.092 (2)	0.850 (5)	0.097 (2)	5.2 (8)
C(23)	1.066 (2)	0.975 (4)	0.140 (2)	5.0 (8)
C(24)	1.023 (2)	0.907 (3)	0.197 (2)	4.1 (7)
C(25)	1.064 (2)	0.866 (3)	0.263 (1)	3.3 (6)*
C(26)	1.160 (2)	0.871 (5)	0.293 (2)	6 (1)
C(27)	1.205 (2)	0.787 (4)	0.246 (2)	5.9 (9)
C(28)	1.156 (2)	0.664 (5)	0.200 (1)	5.3 (9)
C(31)	0.963 (2)	0.438 (4)	0.392 (1)	4.6 (7)
C(32)	0.971 (2)	0.281 (4)	0.425 (2)	5.0 (8)
C(33)	1.030 (2)	0.177 (4)	0.402 (2)	4.9 (8)
C(34)	1.047 (1)	0.240 (3)	0.333 (1)	3.6 (6)
C(35)	1.116 (2)	0.335 (4)	0.336 (2)	4.7 (8)
C(36)	1.167 (2)	0.411 (4)	0.405 (2)	4.7 (7)*
C(37)	1.115 (2)	0.489 (5)	0.448 (2)	6.2 (9)
C(38)	1.030 (2)	0.540 (4)	0.403 (1)	3.9 (7)

[a] Starred values indicate atoms were refined isotropically. Anisotropically refined atoms are given in the form of the isotropic equivalent thermal parameter defined as $(4/3)[a^2B(1,1) + b^2B(2,2) + c^2B(3,3) + ab(\cos\gamma)B(2,1) + ac(\cos\beta)B(1,3) + bc(\cos\alpha)B(2,3)]$.

The molecular structure of **1** consists of a distorted Rh_3 triangle that is capped on each face by a μ_3-S atom. Two Rh–Rh bonds are significantly shorter than the third (Rh(1)–Rh(2) = 2.874 (1) Å, Rh(2)–Rh(3) = 2.904 (2) Å, and Rh(1)–Rh(3) = 3.578 (2) Å). The latter distance is well over the range for a Rh–Rh bond. The Rh(1)–S distances are notably longer than those for Rh(2) and Rh(3). Thus, Rh(1)–S(1) and Rh(1)–S(2) are 2.435 (7) and 2.449 (8) Å, respectively, while the remaining Rh–S distances are shorter and range from 2.330 (3) to 2.384 (4) Å. This distortion is no doubt due to the presence of the three PMe_3 ligands bound to Rh(1) vs COD on Rh(2) and Rh(3).

In order to describe the coordination geometry about each Rh atom, it is initially convenient to disregard the two Rh–Rh bonds. For both Rh(2) and Rh(3), if one considers the centers of the double bonds of each COD and the S atoms, then each Rh atoms is in a distorted-square-planar environment.[18] The overall geometry for Rh(2) and Rh(3) is more complex, however, when the Rh–Rh bonds are included.

(18) For **1**, deviations (Å) from the least-squares planes are as follows. Plane 1: P(1), 0.112 (3); P(2), 0.011 (2); Rh(1), −0.223 (2); S(1), 0.107 (4); S(2), −0.007 (4). Plane 2: Rh(2), 0.390 (2); S(1) −1.196 (3); S(2), −0.362 (3); CT1, 0.120 (1); CT2, 1.049 (1) [CT1 is the midpoint of C(1) and C(8); CT2 is the midpoint of C(4) and C(5)]. Plane 3: Rh(3), −0.377 (2); S(1), −1.112 (3); S(2), 0.260 (4); CT3, −0.027 (2); CT4, −0.968 (1) [CT3 is the midpoint of C(1)′ and C(8)′; CT4 is the midpoint of C(4)′ and C(5)′]. For **2**, deviations (Å) from the least-squares planes are as follows. Plane 1: Ir(1), −0.285 (1); S(1), 0.064 (7); S(2), 0.063 (7); CT1, 0.083 (1); CT2, 0.075 (1) [CT1 is the midpoint of C(14) and C(15); CT2 is the midpoint of C(11) and C(18)]. Plane 2: Ir(2), 0.020 (0); S(1), −0.011 (6); S(2), 0.003 (6); CT3, −0.013 (1); CT4, 0.002 (1) [CT3 is the midpoint of C(24) and C(25); CT4 is the midpoint of C(21) and C(28)]. Plane 3: Ir(3), −0.016 (1); S(1), 0.039 (2); S(2), −0.032 (7); CT5, 0.043 (1); CT6, −0.034 (1) [CT5 is the midpoint of C(31) and C(38); CT6 is the midpoint of C(34) and C(35)].

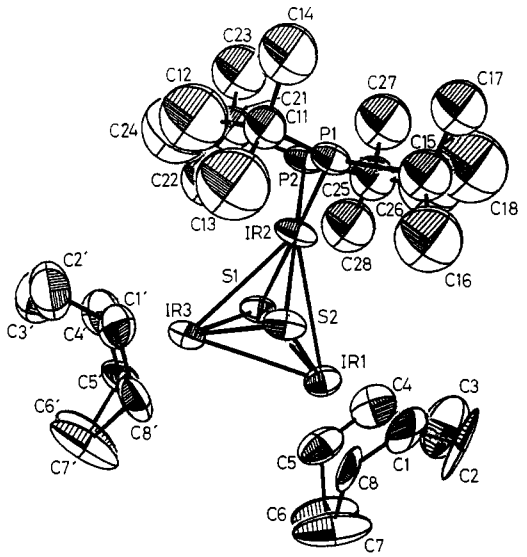

Figure 3. ORTEP view of **4**, showing the atom-numbering scheme. Atoms are shown at the 50% probability level.

For Rh(1), if one again ignores the Rh(1)–Rh(2) bond, then the geometry may be described as a square-based pyramid. Thus, P(1), P(2), S(1), S(2), and Rh(1) are all nearly coplanar, while P(3) forms the vertex of the pyramid. The sum of the angles around Rh(1) making up the distorted square base is 356.9°. The Rh(1)–P(3) distance is considerably larger than the other two. Thus, Rh(1)–P(3) = 2.399 (9) Å, while Rh(1)–P(1) and Rh(1)–P(2) are 2.297 (8) and 2.30 (1) Å, respectively. It seems reasonable to assume that it is P(3) that undergoes the dissociative exchange process observed in the $^{31}P\{^1H\}$ NMR spectrum. The resulting 48-electron cluster then has Rh(1) with a distorted-square-planar geometry (ignoring the Rh–Rh bond). Although the hydride ligand in **1** could not be located in the X-ray structure, it seems reasonable to propose that it bridges the long Rh(1)–Rh(3) interaction, since this part of the molecule is relatively open. However, it is difficult to provide a logical position for it in solution on the basis of the spectroscopic data.

Synthesis of $Ir_3(H)(\mu_3\text{-}S)_2(COD)_3(PMe_3)$ (2). The reaction of $[Ir(COD)Cl]_2$ with $(Me_3Si)_2S$ at −78 °C in THF gives a red solution that darkens to purple upon addition of PMe_3. From this solution, purple crystals of the 50-electron complex $Ir_3(H)(\mu_3\text{-}S)_2(COD)_3(PMe_3)$ (**2**) may be obtained in high yield following crystallization from hexane. In the absence of PMe_3, the complex $Ir_3(H)(\mu_3\text{-}S)_2(COD)_3$ (**3**) may be obtained in 73% yield. The 300-MHz ^1H NMR spectrum of **2** from −80 to +20 °C contains two reasonances assigned to the hydride ligand: δ −10.33 (d, $J_{P\text{-}H}$ = 42.9 Hz), −13.81 (d, $J_{P\text{-}H}$ = 48.6 Hz; relative area ratio 2:1). The resonance at δ −10.33 broadens when the sample is warmed to 40 °C, collapses at 60 °C, and disappears completely at 80 °C. The resonance at δ −13.81 remains unchanged throughout these temperature changes. The separation between the two high-field doublets changes when the spectrum is run at 500 MHz, indicating that a mixture of different isomers exists in solution. The $^{31}P\{^1H\}$ NMR spectrum from −80 to +80 °C consists of two singlets (δ −31.95, −104.14), which is further evidence for the existence of two isomers in solution.

X-ray Structure of 2. The complex crystallizes in the monoclinic space group $P2_1/n$ with four molecules in the unit cell. A view of the molecular structure of **2** is shown in Figure 2. Crystallographic data are collected in Table I, bond lengths and angles are in Table IV, and positional parameters are given in Table V.

Despite the obvious difference in stoichiometry between **1** and **2**, there are some notable similarities in the two structures. If one considers Ir(1) in **2** to be analogous to Rh(1) in **1**, then the COD ligand bound to Ir(1) in **2** merely replaces the two in-plane PMe_3 ligands in **1** (P(1) and P(2)). Thus, there are two relatively short Ir–Ir interactions [Ir(1)–Ir(2) = 2.826 (1), Ir(2)–Ir(3) = 2.809 (2) Å] and one considerably longer [Ir(1)–Ir(3) = 3.614 (1) Å]. The coordination geometries about Ir(2) and Ir(3) may be considered to be distorted square planar if one ignores the Ir–Ir bonds. The geometry of Ir(1) can be thought of as that of a square-based pyramid in which the midpoints of the double bonds of the COD ligand and the S atoms form the base and P the vertex.

Unlike those in **1**, the Ir–S distances in **2** all fall within a fairly narrow range. Thus, Ir(1)–S(1) and Ir(1)–S(2) at 2.374 (6) and 2.391 (6) Å are only slightly longer than the other Ir–S distances, which range from 2.356 (7) to 2.367 (7) Å. The presence of three good σ-donor PMe_3 ligands bound to Rh(1) in **1** vs one on Ir(1) in **2** is an important factor that must affect the electronic environment of the metals in the two compounds. Thus, Rh(1) is probably considerably more electron rich than Ir(1), and this difference may be responsible for the differences in the Rh(1)–S and Ir(1)–S bond distances. The Ir(1)–P distance is 2.394 (9) Å, which is similar to the Rh(1)–P(3) distance in **1** [2.399 (9) Å]. As for **1**, the unique hydride ligand in **2** could not be located in the X-ray structure. We propose that it spans the long Ir(1)–Ir(3) interaction in the solid state in a manner similar to that suggested for **1**.

Synthesis of $Ir_3(H)(\mu\text{-}_3\text{-}S)_2(COD)_3$ (3). The reaction of $[Ir(COD)Cl]_2$ with either H_2S or NaSH in methanol at −78 °C gives a red solution on warming to room temperature. From this solution, red crystalline $Ir_3(H)(\mu_3\text{-}S)_2(COD)_3$ (**3**) may be obtained in high yield by recrystallization from toluene. As noted above, this compound may also be prepared from $(Me_3Si)_2S$ and $[Ir(COD)Cl]_2$. The ^1H NMR spectrum of **3** has resonances assigned to the COD ligands in addition to a resonance upfield of Me_4Si (δ −21.48 s) assigned to the hydride ligand. Spectroscopic data were not structurally diagnostic, and we did not obtain crystals of **3** suitable for X-ray diffraction studies. However, it seems reasonable to assume that the structure of **3** is similar to that of the Rh analogue $Rh_3(H)(\mu_3\text{-}S)_2(COD)_3$, which we described recently.[4] Both complexes have formally 48-electron counts.

Synthesis of $Ir_3(H)(\mu_3\text{-}S)_2(COD)_2(t\text{-}Bu_2PH)_2$ (4). Since the 48-electron complex **3** reacts with excess PMe_3 to give 50-electron **2** in good yield (Scheme II), we have also investigated the reactions of **3** with other phosphines. It seems likely that the formation

Table VI. Selected Bond Lengths (Å) and Angles (deg) for **4**[a]

Ir(1)–Ir(2)	3.086 (1)	Ir(2)–P(2)	2.277 (5)
Ir(1)–Ir(3)	2.938 (1)	Ir(3)–S(1)	2.322 (5)
Ir(2)–Ir(3)	3.020 (0)	Ir(3)–S(2)	2.326 (5)
Ir(1)–S(1)	2.318 (5)	Ir(3)–C(1)′	2.13 (3)
Ir(1)–S(2)	2.333 (6)	Ir(3)–C(4)′	2.13 (3)
Ir(1)–C(1)	2.14 (2)	Ir(3)–C(5)′	2.13 (2)
Ir(1)–C(4)	2.14 (3)	Ir(3)–C(8)′	2.13 (2)
Ir(1)–C(8)	2.11 (2)	P(1)–C(11)	1.85 (3)
Ir(2)–S(1)	2.364 (5)	P(1)–C(15)	1.91 (3)
Ir(2)–S(2)	2.367 (4)	P(2)–C(21)	1.90 (3)
Ir(2)–P(1)	2.275 (5)	P(2)–C(25)	1.98 (3)
Ir(2)–Ir(1)–Ir(3)	60.11 (1)	S(2)–Ir(2)–P(2)	174.68 (8)
Ir(1)–Ir(3)–Ir(2)	62.37 (1)	P(1)–Ir(2)–P(2)	93.56 (8)
Ir(1)–Ir(2)–Ir(3)	57.52 (1)	S(1)–Ir(3)–S(2)	84.41 (8)
Ir(2)–Ir(1)–S(1)	49.42 (5)	Ir(1)–S(1)–Ir(2)	82.45 (7)
Ir(2)–Ir(1)–S(2)	49.43 (5)	Ir(1)–S(1)–Ir(3)	78.57 (7)
Ir(3)–Ir(1)–S(1)	50.78 (6)	Ir(1)–S(1)–S(2)	48.04 (6)
Ir(3)–Ir(1)–S(2)	50.79 (6)	Ir(2)–S(1)–Ir(3)	80.22 (7)
S(1)–Ir(1)–S(2)	84.34 (8)	Ir(2)–S(1)–S(2)	48.73 (6)
S(1)–Ir(2)–S(1)	48.12 (5)	Ir(3)–S(1)–S(2)	47.85 (6)
Ir(1)–Ir(2)–S(2)	48.49 (6)	Ir(1)–S(2)–Ir(2)	82.08 (7)
Ir(1)–Ir(2)–P(1)	128.52 (6)	Ir(1)–S(2)–Ir(3)	78.19 (7)
Ir(1)–Ir(2)–P(2)	126.67 (7)	Ir(1)–S(2)–S(1)	47.62 (6)
Ir(3)–Ir(2)–S(1)	49.28 (5)	Ir(2)–S(2)–Ir(3)	80.10 (7)
Ir(3)–Ir(2)–S(2)	49.36 (6)	Ir(2)–S(2)–S(1)	48.67 (6)
Ir(3)–Ir(2)–P(1)	124.99 (6)	Ir(3)–S(2)–S(1)	47.75 (6)
Ir(3)–Ir(2)–P(2)	127.36 (7)	Ir(1)–Ir(3)–S(1)	50.65 (6)
S(1)–Ir(2)–S(2)	82.60 (7)	Ir(1)–Ir(3)–S(2)	51.02 (6)
S(1)–S(2)–P(1)	173.90 (8)	Ir(2)–Ir(3)–S(1)	50.50 (5)
S(1)–Ir(2)–P(2)	92.21 (8)	Ir(2)–Ir(3)–S(2)	50.54 (5)
S(2)–Ir(2)–P(1)	91.67 (8)		

[a] Numbers in parentheses are estimated standard deviations in the least significant digits. A complete listing is available in the supplementary material.

Table VII. Positional Parameters for **4**[a]

atom	x	y	z	B, Å²
Ir(1)	0.19027 (7)	0.17626 (4)	0.76284 (8)	3.71 (2)
Ir(2)	−0.01432 (7)	0.27322 (5)	0.56630 (7)	3.68 (2)
Ir(3)	0.23762 (7)	0.31908 (4)	0.82118 (8)	3.43 (2)
S(1)	0.0542 (4)	0.2681 (3)	0.8087 (5)	3.3 (1)
S(2)	0.2200 (4)	0.2422 (3)	0.6221 (5)	3.7 (1)
P(1)	−0.0565 (5)	0.2792 (3)	0.3387 (5)	3.6 (1)
P(2)	−0.2363 (4)	0.3006 (3)	0.5325 (5)	3.7 (1)
C(1)′	0.356 (2)	0.381 (1)	0.781 (3)	5.8 (7)
C(1)	0.264 (2)	0.084 (1)	0.673 (2)	6.7 (7)
C(2)′	0.331 (3)	0.454 (1)	0.828 (3)	9 (1)
C(2)	0.207 (3)	0.024 (1)	0.681 (3)	10.3 (9)
C(3)	0.115 (4)	0.035 (2)	0.757 (4)	11 (1)
C(3)′	0.273 (4)	0.467 (2)	0.933 (3)	10 (1)
C(4)′	0.211 (3)	0.408 (1)	0.953 (3)	6.8 (8)
C(4)	0.112 (2)	0.109 (1)	0.837 (2)	6.4 (7)
C(5)	0.227 (3)	0.139 (1)	0.952 (2)	6.3 (7)
C(5)′	0.295 (2)	0.359 (1)	1.039 (2)	5.7 (7)
C(6)	0.368 (3)	0.103 (2)	1.015 (3)	10 (1)
C(6)′	0.449 (3)	0.361 (2)	1.120 (3)	10 (1)
C(7)	0.452 (3)	0.098 (2)	0.931 (3)	10.6 (9)
C(7)′	0.523 (3)	0.356 (2)	1.036 (3)	10 (1)
C(8)′	0.445 (2)	0.332 (1)	0.871 (2)	5.7 (6)
C(8)	0.372 (2)	0.116 (1)	0.785 (2)	5.3 (6)
C(11)	0.018 (2)	0.347 (1)	0.307 (2)	4.8 (5)*
C(12)	0.003 (4)	0.409 (2)	0.409 (4)	13 (1)*
C(13)	0.167 (3)	0.346 (2)	0.369 (3)	13.6 (9)*
C(14)	−0.041 (3)	0.358 (2)	0.148 (3)	9.1 (9)*
C(15)	−0.047 (3)	0.196 (1)	0.222 (3)	7.5 (7)*
C(16)	0.094 (4)	0.168 (2)	0.262 (4)	12 (1)*
C(17)	−0.105 (3)	0.203 (1)	0.060 (3)	7.8 (7)*
C(18)	−0.161 (5)	0.158 (3)	0.215 (5)	16 (2)*
C(21)	−0.279 (3)	0.386 (1)	0.618 (3)	7.2 (7)*
C(22)	−0.238 (4)	0.382 (2)	0.778 (4)	11 (1)*
C(23)	−0.432 (4)	0.409 (2)	0.563 (4)	11 (1)*
C(24)	−0.191 (5)	0.433 (3)	0.642 (5)	16 (2)*
C(25)	−0.330 (3)	0.226 (1)	0.538 (3)	7.6 (7)*
C(26)	−0.311 (5)	0.171 (2)	0.437 (5)	15 (2)*
C(27)	−0.486 (4)	0.244 (2)	0.475 (4)	12 (1)*
C(28)	−0.291 (4)	0.222 (2)	0.696 (4)	12 (1)*
C(31)	0.250 (4)	0.983 (2)	0.199 (4)	11 (1)*
C(32)	0.367 (3)	1.018 (2)	0.317 (3)	9.8 (9)*
C(33)	0.443 (3)	0.981 (1)	0.445 (3)	7.4 (7)*

[a] Starred values indicate atoms were refined isotropically. Anisotropically refined atoms are given in the form of the isotropic equivalent thermal parameter defined as $(4/3)[a^2B(1,1) + b^2B(2,2) + c^2B(3,3) + ab(\cos\gamma)B(1,2) + ac(\cos\beta)B(1,3) + bc(\cos\alpha)B(2,3)]$.

of **2** from **3** is in part made possible by the small size of the PMe_3 ligand, since the reaction of **2** with the bulky secondary phosphine (t-Bu_2PH) results in complete loss of one COD ligand and the formation of only a bis(phosphine) complex $Ir_3(H)(\mu_3\text{-}S)_2(COD)_2(t\text{-}Bu_2PH)_2$ (**4**), which is still a 48-electron cluster. We recently described the Rh analogue of **4**, $Rh_3(H)(\mu_3\text{-}S)_2(COD)_2(t\text{-}Bu_2PH)_2$,[4] which has a similar structure in the solid state. Spectroscopic data for **4** are in accord with the structure determined by X-ray crystallography. Thus, the IR spectrum contains a weak peak at 2265 cm^{-1} assigned to $\nu_{P\text{-}H}$. The ^1H NMR spectrum contains resonances assigned to the COD and t-Bu_2PH ligands in addition to a hydride signal at δ −27.92 (t, $^2J_{P\text{-}H}$ = 19.8 Hz). The $^{31}P\{^1H\}$ NMR spectrum shows a singlet at δ 54.65.

X-ray Structure of 4. Molecules of **4** crystallize in the triclinic space group $P\bar{1}$ with two independent molecules in the unit cell. A view of **4** is shown in Figure 3. Key bond lengths and angles for the compound are given in Table VI. Positional parameters are in Table VII.

The structural parameters are similar to those of $Rh_3(H)(COD)_2(\mu_3\text{-}S)_2(t\text{-}Bu_2PH)_2$, and the Ir_3S_2 core is similar to that found in **2**. Interestingly, compared to those for **1** and **2**, the Ir–Ir distances for **4** are all approximately equal (3.086 (1), 2.938 (1), 3.020 (1) Å) and may all be considered to be bonding. Again, as for **1** and **2**, the unique hydride ligand could not be located in the X-ray structure. We propose that in the solid state it bridges the Ir(1)–Ir(3) bond, since it is the least sterically inhibited part of the molecule.

Experimental Section

All reactions were performed under oxygen-free nitrogen or under vacuum. Microanalyses were by the Schwarzkopf Microanalytical Laboratory, Woodside, NY. Hexane, THF, and diethyl ether were dried over sodium and distilled from sodium benzophenone ketyl under nitrogen before use. Toluene was freshly distilled from sodium metal under nitrogen. $[Ir(COD)Cl]_2$,[19] $[Rh(COD)Cl]_2$,[20] t-Bu_2PH,[21] and $(Me_3Si)_2S$[22] were prepared by the literature procedures. Melting points were in sealed capillaries under nitrogen (1 atm) and are uncorrected. Instruments used were as follows. IR: Perkin-Elmer 1330. NMR: Varian EM-390 (^1H, 90 MHz), FT-80 (^{31}P, 32.384 MHz), GE QE-300 (^1H, ^{31}P), GE 500 (^1H). IR spectra were as Nujol mulls or in solution (matched KBr or CaF_2 cells). NMR spectra were recorded in C_6D_6 at ambient temperature (unless otherwise stated) and are referenced to Me_4Si (δ 0.0, ^1H) and 85% H_3PO_4(aq) (δ 0.0, ^{31}P, downfield is positive). Satisfactory elemental analyses were obtained on **1–4** (C, H).

Synthesis of $Rh_3(H)(\mu_3\text{-}S)_2(COD)_3$. This compound may also be prepared from NaSH and $[Rh(COD)Cl]_2$.[4] A solution of $[Rh(COD)Cl]_2$ (0.20 g, 0.41 mmol) in THF (40 mL) was cooled (−78 °C), and $(Me_3Si)_2S$ (0.20 mL, 0.95 mmol) was added. The solution turned light orange immediately and was stirred (3 h) under nitrogen. While warming to room temperature, the solution turned dark red. Volatile materials were removed under vacuum. The residue was extracted into hexane (40 mL) and the solution filtered and reduced in volume (15 mL). Cooling (−40 °C) gave bright red crystals of $Rh_3(H)(\mu_3\text{-}S)_2(COD)_3$, which were collected and dried under vacuum. Yield: 0.17 g (77%). The spectroscopic properties of this compound are reported in ref 4.

Synthesis of $Ru_3(H)(\mu_3\text{-}S)_2(COD)_2(PMe_3)_3$ (1). Hexamethyldisilthiane (0.04 mL, 0.19 mmol) and a 3 molar excess of PMe_3 (0.10 mL, 1.01 mmol) were added to a solution of $[Rh(COD)Cl]_2$ (0.10 g, 0.20 mmol) in THF (40 mL) at −78 °C. The mixture was warmed slowly to room temperature, turning from yellow to dark red (3 h). Volatile materials were removed under vacuum, the residue was extracted into hexane, and the solution was filtered and evaporated (10 mL). Cooling (−10 °C) yielded dark red crystals, which were collected and dried under vacuum. Yield: 0.09 g (82%). Mp: 131–134 °C. ^1H NMR (C_7D_8, −20 °C, δ 0.0 at 300 MHz): δ 4.69 (m, 8 H, C*H*), 2.69 (m, 16 H, CH_2), 1.43 (d, 9 H, P*Me*$_3$, $J_{P\text{-}H}$ = 6.0 Hz), 1.03 (d, 18 H, *PMe*$_3$, $J_{P\text{-}H}$ = 7.5 Hz), −5.77 (dt, 1 H, Rh–*H*, $J_{Rh\text{-}H}$ = 11.5 Hz, $J_{P\text{-}H}$ = 184.8 Hz). $^{31}P\{^1H\}$ NMR (C_7D_8, −50 °C): δ 2.89 (dd, *P*Me$_3$, $^1J_{Rh\text{-}P}$ = 118.7 Hz), −5.62 (dd, *P*Me$_3$, $^1J_{Rh\text{-}P}$ = 118.2 Hz, $^2J_{P\text{-}P}$ = 19.6 Hz), −40 ($\Delta w_{1/2}$ = 360 Hz). IR (Nujol mull, NaCl): 1323 m, 1296 m, 1275 m, 1236 w, 1207 w, 1173 w, 1146 w, 1074 w, 1009 w, 989 w, 941 s, 835 m, 847 m, 815 m, 793 w, 725 m, 677 m, 671 w cm^{-1}.

Synthesis of $Ir_3(H)(\mu_3\text{-}S)_2(COD)_3(PMe_3)$ (2). Hexamethyldisilthiane (0.06 mL, 0.29 mmol) and a 3 molar excess of PMe_3 (0.10 mL, 1.01 mmol) were added to a solution of $[Ir(COD)Cl]_2$ (0.20 g, 0.30 mmol) in THF (40 mL) at −78 °C. The mixture was warmed slowly to room temperature, turning from orange to purple after 3 h. Volatile materials were removed under vacuum, and the residue was extracted into hexane (30 mL). The solution was filtered and evaporated (10 mL). Cooling (−10 °C) gave purple crystals, which were collected and dried under vacuum. Yield: 0.12 g (58%). Mp: 212–215 °C. ^1H NMR (C_6D_6, −20 °C): δ 4.66 (m, 12 H, C*H*), 2.56 (m, 24 H, CH_2); three peaks (relative intensities in parentheses) for the PMe_3 ligands δ 0.93 (1), 0.91 (2), 0.88 (1); δ −10.33 (d, Ir–*H*, $^2J_{P\text{-}H}$ = 42.9 Hz), −13.81 (d, Ir-*H*, $^2J_{P\text{-}H}$ = 48.6 Hz) (relative areas for the Ir–H signals are 2:1, respectively). $^{31}P\{^1H\}$ NMR (C_6D_6, −50 °C): δ −31.95 (s, *P*Me$_3$), −104.14 (s, *P*Me$_3$). IR (Nujol mull, NaCl): 1315 w, 1271 w, 1255 w, 1225 w, 1198 w, 1143 w, 1061 w, 992 w, 943 m, 883 m, 866 w, 740 w, 665 w, 594 w cm^{-1}.

Synthesis of $Ir_3(H)(\mu_3\text{-}S)_2(COD)_3$ (3). (i) From NaSH. Two equivalents of NaSH, as a solution in MeOH (1.2 mL of a 1.31 M solution), was added to a stirred solution of $[Ir(COD)Cl]_2$ (0.53 g, 0.79 mmol) in MeOH (30 mL) at −78 °C. The solution was allowed to warm to room temperature over a period of 3 h, during which the color changed from orange to dark red. The solution was allowed to stir for a further 20 h at room temperature. Volatile materials were then removed under vacuum, and the resulting red residue was extracted with toluene (2 × 20 mL) and the extract filtered. The extract was concentrated (15 mL) and cooled (−20 °C) for 20 h to yield a dark red microcrystalline product

(19) Herde, J. L.; Lambert, J. C.; Senoff, C. V. *Inorg. Synth.* **1974**, *15*, 18.
(20) Giordano, G.; Crabtree, R. H. *Inorg. Synth.* **1979**, *19*, 218.
(21) Hoffman, H.; Schellenbeck, P. *Chem. Ber.* **1966**, *99*, 1134.
(22) Armitage, D. A.; Clark, M. J.; Sinden, A. W.; Wingfield, J. N.; Abel, E. W. *Inorg. Synth.* **1974**, *15*, 210.

isolated by decantation of the supernatant liquid. The product is air stable over a period of hours. Yield: 0.34 g (69%). MP: the product darkens over the range 150–155 °C and decomposes above 250 °C. ^{1}H NMR (C_6D_6, 300 MHz): δ 4.61 (m, 4 H, C*H*), 2.05 (m, 8 H, CH_2), −21.48 (s, 1 H, Ir−*H*). IR (KBr disk): 2950 w, 2920 w, 2850 w, 2810 w, 1440 w, 1310 w, 1250 m, 1170 w, 1140 w, 1080 m, br, 1010 m, br, 860 w, 795 s, 720 w, 460 w, 415 w cm^{-1}.

(ii) From H_2S. H_2S (1 atm) was bubbled slowly through a suspension of $[Ir(COD)Cl]_2$ (0.10 g, 0.15 mmol) in methanol (30 mL) at room temperature. After 1 h the solution turned dark red in color. Volatile materials were removed under vacuum to leave a dark red residue, which was washed with hexane (20 mL). Extraction of the residue with toluene (30 mL) gave a dark red solution that gave crystalline **3** upon cooling (−20 °C). Yield: 0.32 g (65 %).

(iii) From $(Me_3Si)_2S$. Two equivalents of $(Me_3Si)_2S$ (0.06 mL, 0.29 mmol) was added to a suspension of $[Ir(COD)Cl]_2$ (0.1 g, 0.15 mmol) in THF (40 mL) at −78 °C. Upon warming to room temperature (3 h), the solution turned deep red. Volatile materials were removed under vacuum, and the resulting red residue was extracted with hexane (50 mL) and the extract filtered. The solution was concentrated (10 mL) and cooled (−40 °C, 24 h) to yield a dark red crystalline material. Yield: 0.07 g (73%).

Synthesis of $Ir_3(H)(\mu_3\text{-}S)_2(COD)_2(t\text{-}Bu_2PH)_2$ (4). Six equivalents of t-Bu_2PH (0.25 mL, 1.82 mmol) was added to a solution of **3** (0.21 g, 0.22 mmol) in toluene (40 mL) at room temperature. The bright red solution was then refluxed (66 h), after which it became dark brown. Volatile materials were removed under vacuum to yield a yellow-brown residue, which was extracted into hexane (2 × 30 mL), and the extract was filtered to yield a bright yellow solution. Concentration under vacuum (20 mL) and cooling (−20° C) for 20 h gave bright orange prisms of **4**, which were collected and dried under vacuum. The product is stable in air for several days. Yield: 0.13 g (53%). MP: the compound loses crystallinity at 118–124 °C and decomposes further to a black residue above 295 °C. ^{1}H NMR (C_6D_6, 300 MHz): δ 4.62 (m, 4 H, C*H*), 4.42 (m, 4 H, C*H*), 4.18 (dd, 2 H, $^1J_{P-H}$ = 331.2 Hz, $^2J_{P-H}$ = 17.5 Hz, P*H*), 4.11 (d, 1 H, $^1J_{P-H}$ = 331.2 Hz, P*H*), 2.18 (br m, 16 H, CH_2), 1.40 (d, 18 H, $^2J_{P-H}$ = 14.0 Hz, t-Bu−P), 1.22 (d, 18 H, $^2J_{P-H}$ = 14.0 Hz, *t-Bu*−P), −27.92 (t, 1 H, $^2J_{P-H}$ = 19.0 Hz, μ-*H*). ^{31}P {^{1}H} NMR: δ 54.65 (s). IR (KBr disk): 2960 w, 2945 w, 2900 m, 2840 m, 2800 m, 2265 m, 1465 m, 1455 w, 1435 m, 1415 w, 1380 m, 1350 m, 1305 m, 1280 w, 1250 m, 1220 w, 1190 w, 1170 w, 1140 w, 1090 m, br, 1010 m, 990 w, 960 w, 930 w, 895 w, 870 m, 800 m, 570 m, 510 w, 480 m, 465 m, 390 w cm^{-1}.

X-ray Experimental Section

Data were collected on an Enraf-Nonius CAD-4 diffratometer at 24 ± 2 °C using graphite-monochromated Mo Kα radiation. All calculations were performed on a PDP 11/44 computer using the Enraf-Nonius software package SDP-PLUS.[23] For each structure, the data were corrected for Lorentz and polarization effects. The structures were solved by direct methods (MULTAN)[24] and successive cycles of difference Fourier maps followed by least-squares refinement. Data with intensities less than $3\sigma(I)$ were excluded, and a non-Poisson contribution weighting scheme with an instability factor P set at 0.08 for **1** and **2** and 0.07 for **4** was used in the final stages of refinement.[25]

Compound 1. Crystals of **1** were grown by slow cooling of a hexane solution (−10 °C). A suitable black parallelepiped was mounted in a thin-walled glass capillary and sealed under nitrogen. No hydrogen atoms were located in the structure, but their contributions were included in the refinements. All the Rh, P, and S atoms were refined anisotropically, while most of the carbon atoms were refined with isotropic thermal parameters.

Compound 2. Crystals of **2** were grown by slow cooling of a hexane solution (−10 °C). A suitable purple prism was mounted in a thin-walled glass capillary and sealed under vacuum. No hydrogen atoms were located in the structure, but their contributions were included in the refinements. All atoms except for C(25) and C(36) were refined with anisotropic thermal parameters.

Compound 4. Crystals of **4** were grown by slow cooling of a hexane solution (−20 °C). A suitable bright orange prism was mounted in a thin-walled glass capillary and sealed under nitrogen. All Rh, P, and S atoms and C atoms of the COD units were refined anisotropically, while the carbon atoms of the t-Bu groups were refined isotropically. No hydrogen atoms were located in the structure, but their contributions were included in the refinements. Scattering factors were taken from ref 26. Supplementary material for all three structures is available.[27]

Acknowledgments. We thank the Robert A. Welch Foundation (Grant F-816), the National Science Foundation (Grant CHE-8517759), and the Texas Advanced Technology Research Program for support. R.A.J. Thanks the Alfred P. Sloan Foundation for a fellowship (1985–1989).

Supplementary Material Available: Complete listings of bond lengths and angles, thermal parameters, and crystal and structure parameters for **1**, **2**, and **4** (19 pages); tables of observed and calculated structure factors for **1**, **2**, and **4** (85 pages). Ordering information is given on any current masthead page.

(23) *SDP-PLUS*, 4th ed.; B. A. Frenz and Associates: College Station, TX 77840, 1981.

(24) Germain, G.; Main, P.; Wolfson, M. M. *Acta Crystallogr., Sect. A: Cryst. Phys. Diffr. Theor. Gen. Crystallogr.* **1971**, *A27*, 368.

(25) P is used in the calculation of $\sigma(I)$ to downweight intense reflections in the least-squares refinement. The function minimized was $\sum w(|F_o|-|F_c|)^2$, where $w = 4(F_o)^2/[\sum(F_o)^2]^2$, $[\sum(F_o)^2] = [S^2(C + R^2B) + (P(F_o)^2)^2]/Lp^2$, and S is the scan rate, C is the total integrated peak count, R is the ratio of scan time to background counting time, B is the total background count, and Lp is the Lorentz–polarization factor.

(26) *International Tables for X-ray Crystallography*; Kynoch: Birmingham, England, 1974; Vol. IV.

(27) See paragraph at the end of the paper regarding supplementary material.